Input Impedance of a Coaxial Line Probe Feeding a Circular Waveguide in the TM_{01} Mode

R. H. MACPHIE, SENIOR MEMBER, IEEE, M. OPIE, AND C. R. RIES

Abstract—**By means of the conservation of complex power technique (CCPT), a formally exact full-wave solution is given for the case of a coaxial line probe feeding a circular waveguide for TM_{01} modal excitation. The overall scattering matrix of the coaxial line probe–circular waveguide system is deduced and numerical results for the impedance as "seen" by the coaxial line are presented and compared with experimental results obtained in the 9.0–11.5 GHz frequency range.**

I. Introduction

Coaxial transmission line discontinuities received early attention in a classic paper [1] by Whinnery, Jamieson, and Robbins, who used full-wave modal analysis to obtain the equivalent shunting capacitances for a variety of such junctions. About a quarter of a century later, Risley [2] [3], by combining modal analysis and the Rayleigh–Ritz variational technique, considered the junction of a coaxial line with a larger circular waveguide.

A natural sequel to Risley's work is to let the coaxial line's center conductor extend into the circular guide (as in Fig. 1), thereby creating an axial probe which efficiently excites the TM_{01} mode in the circular guide. The present paper provides a full-wave solution to this problem; the conservation of complex power technique (CCPT) [4]–[6] and the generalized scattering matrix technique [7] are used and numerical results are presented for a variety of cases. Moreover, experimental results for a circular guide with a TM_{01} mode cutoff frequency of 8.14 GHz fed by an axial probe and a 50 Ω semirigid coaxial cable show quite good agreement with the numerical results obtained by the CCPT.

II. Solution of the Scattering Problem by the Conservation of Complex Power Technique

Fig. 1 illustrates the geometry of the coaxial line–circular waveguide junction. We assume that the permittivities are ϵ_1 for $z<0$, ϵ_0 for $z>0$ and that $\mu=\mu_0$ everywhere. There are, effectively, three waveguides, i.e., the small coaxial line for $z<0$ (guide 1), the larger coaxial guide for $0<z<h$ (guide 2, the probe antenna region), and the circular guide for $z>h$ (guide 3). There are two junctions, at $z=0$ (junction A) and at $z=h$ (junction B), at which scattering will take place. In particular we are concerned with the scattering of a TEM (TM_{00}) field incident from the small coaxial line and with deducing the effective load impedance Z_L at $z=0$.

At each junction (A and B) it is straightforward, using the CCPT, to obtain the scattering matrices $[S_A]$ and $[S_B]$ for the modal amplitudes of the TM_{0m} fields excited by a TEM coaxial line field incident from guide 1. The analytical expressions for the elements of the E-field mode matching matrices $[E_A]$ and $[E_B]$, necessary to deduce $[S_A]$ and $[S_B]$, are given in the Appendix. Using $[S_A]$ and $[S_B]$ with the generalized scattering matrix technique [7] we can obtain an expression for the scattering matrix $[S_{11}^c]$ for the overall cascaded junction which relates the TM_{0m} mode amplitudes backscattered in guide 1 to those incident from the same guide:

$$[S_{11}^c]=[S_{11}^A]+[S_{12}^A][L_2][S_{22}^B][G_1][L_2][S_{21}^A] \tag{1}$$

where

$$[G_1]^{-1}=[I]-[L_2][S_{22}^A][L_2][S_{22}^B] \tag{2}$$

and $[L_2]$ is the diagonal equivalent transmission line matrix for guide 2 whose elements, for TM_{0m} modes, are given in the Appendix; $[I]$ is the identity matrix.

Of particular interest is the TEM reflection coefficient in guide 1, given by

$$\Gamma=S_{11,mn}^c\Big|_{m=n=0}=S_{11,00}^c \tag{3}$$

i.e., the 00th element of $[S_{11}^c]$. From Γ we obtain the TEM normalized load impedance

$$\bar{Z}_L=\frac{Z_L}{Z_0}=\frac{1+\Gamma}{1-\Gamma} \tag{4}$$

where Z_0 is the coaxial line's characteristic impedance.

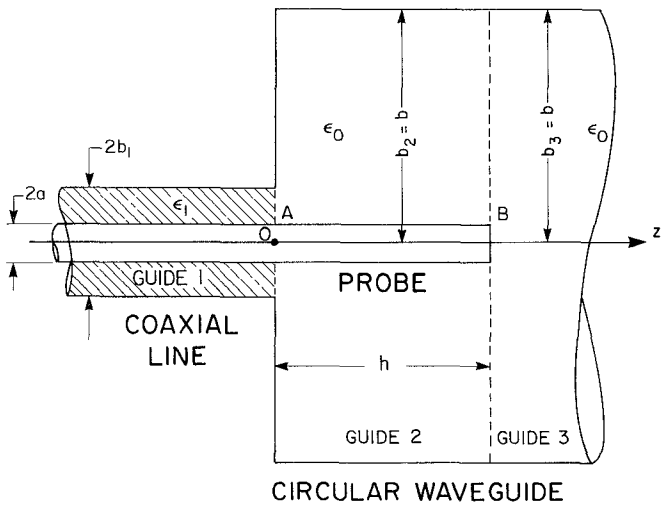

Fig. 1 A circular waveguide fed by a coaxial line probe for TM_{01} mode excitation

TABLE I
CONVERGENCE OF $\Gamma=S_{11,00}^c$ FOR THE CASE OF $\epsilon_1=2.00\epsilon_0$, $\epsilon_2=\epsilon_0$, $a_1=0.456$ mm, $b_1=1.50$ mm, $b_2=b_3=14.1$ mm, $f=10$ GHz

$N_2=N_3$	N_1	
	3	4
30	$\Gamma=0.16650-j0.34122$	$\Gamma=0.16658-j0.34114$
40	$\Gamma=0.16653-j0.34113$	$\Gamma=0.16660-j0.34105$

III. Numerical Results

In normal practice the outer radius b_1 of the coaxial line is very much smaller than the radius b of the circular guide (see Fig. 1). In order to avoid the relative convergence problem [7] at junction A, in the numerical calculations we typically used three

Manuscript received May 22, 1989; revised October 3, 1989. This work was supported by the Natural Sciences and Engineering Research Council (NSERC), Ottawa, Canada, under Grant A-2176.

R. H. MacPhie is with the Department of Electrical Engineering, University of Waterloo, Waterloo, Ont., Canada N2L 3G1.

M. Opie is with the Department of Electrical Engineering, University of Manitoba, Winnipeg, Man., Canada R3T 3G1.

C. E. Ries is with the Department of Electrical and Computer Engineering, McMaster University, Hamilton, Ont., Canada L8S 4L7.

IEEE Log Number 8933001.

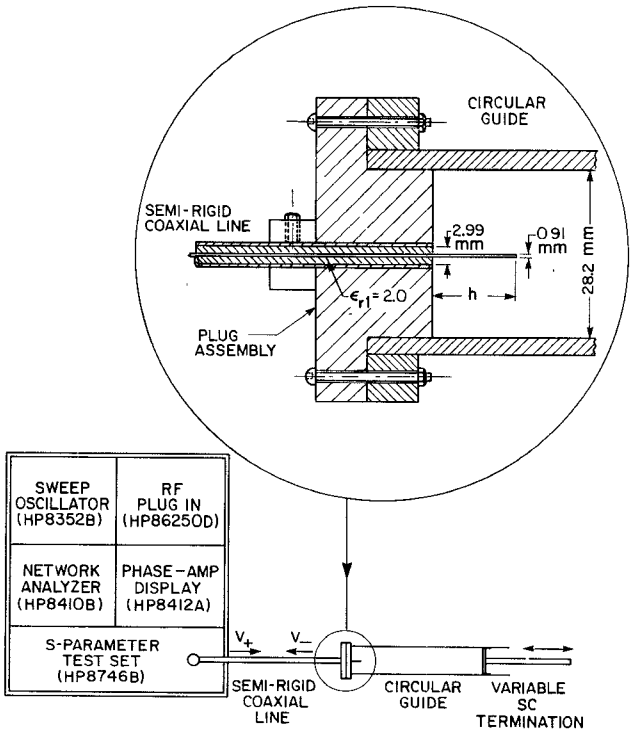

Fig. 2. The experimental setup; a circular guide ($f_{c,01}^{TM} = 8.14$ GHz) fed by a $Z_0 = 50\ \Omega$ semirigid coaxial line probe.

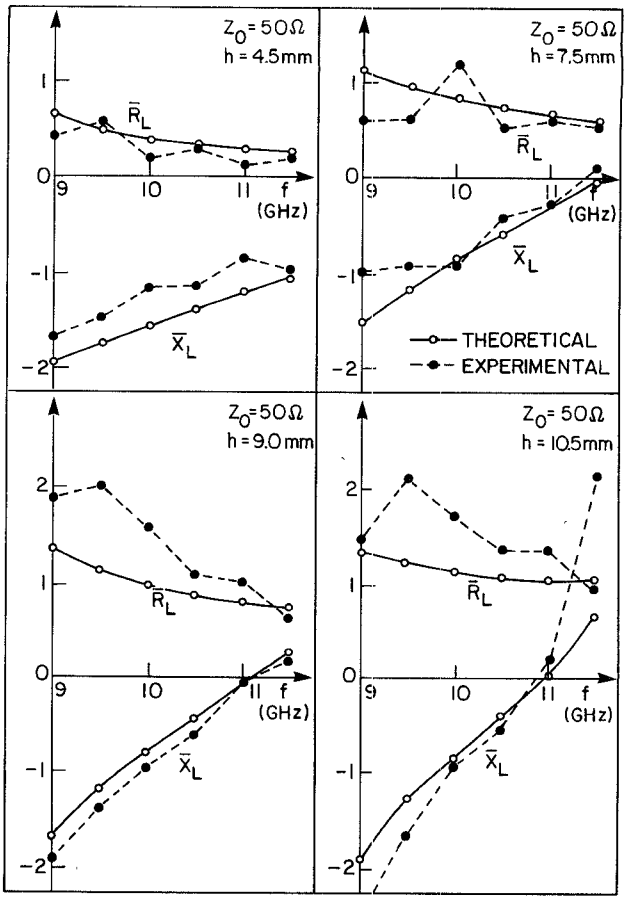

Fig. 3. Comparison of experimental and theoretical results for the experimental setup of Fig. 2: normalized load impedance versus frequency for probe lengths of $h = 4.5$ mm, $h = 7.5$ mm, $h = 9.0$ mm, and $h = 10.5$ mm.

modes in guide 1 ($N_1 = 3$) and $N_2 = 200$ modes in guide 2 to compute the scattering matrix $[S_{11}^A]$ in (1); moreover, in all cases $N_2/N_1 \geq b/b_1$, to avoid relative convergence. Fortunately $[S_{11}^A]$ is of size $N_1 \times N_1$ and to calculate it [4] one needs to invert a matrix of size 3×3 only. Moreover if only the TM_{01} mode can propagate, then most of the $N_2 = 200$ mode fields transmitted into guide 2 will have negligible amplitude when they reach junction B at $z = h$. As a result, in our computations involving $[S_B]$ we typically set $N_2 = N_3 = 40$. To illustrate the accuracy of such a computing strategy we calculated $\Gamma = S_{11,00}^c$ for a typical case with $N_1 = 3$, 4 and $N_3 = 30$, 40. The results are shown in Table I and indicate that the accuracy is probably better than 0.1 percent when $N_1 = 3$ and $N_3 = 40$.

The particular case considered in Table I is one that was realized in practice. The coaxial line's parameters correspond to those of the $Z_0 = 50\ \Omega$ semirigid coaxial cable with $a = 0.456$ mm and $b_1 = 1.50$ mm. The circular guide with $b_3 = b = 14.1$ mm was brass tubing with a 1.25 in OD, a wall thickness of 0.075 in, and a cutoff frequency for the TM_{01} mode of 8.14 GHz. A movable short-circuited (S.C.) termination was used, as shown in the schematic diagram of the experimental setup in Fig. 2. Then Deschamps's method [8] yielded the reflection coefficient Γ and hence, via (4), the normalized load impedance $\bar{Z}_L$ for a variety of frequencies and probe lengths h.

The theoretical and experimental results are given in Fig. 3. Their agreement is reasonably good except at the lower frequencies ($f < 10.0$ GHz), where the TM_{01} mode in the circular guide is close to its cutoff frequency (8.14 GHz). We note that for a probe length of 10.5 mm and at a frequency of about 10.95 GHz, the theory predicts that $\bar{Z}_L \approx 1$, a matched load. Our experimental results at 11.0 GHz indicated a $\bar{Z}_L = 1.34 + j0.22$, for which $|\Gamma| = 0.18$, quite close to a matched load.

Additional numerical results are given in Fig. 4, where the coaxial line with $\epsilon_{r1} = 2.26$ (polyethylene) has a characteristic impedance $Z_L = 75\ \Omega$. The probe diameter is $a = 0.01\lambda$ (λ is the free-space wavelength) and the normalized probe length h/λ is varied, with b as a parameter. For $b = 0.25\lambda$ no mode can propagate in the circular guide, which therefore would appear to the central coaxial guide's propagating TEM mode as a capacitive load $Z_{LB} = -j|X_{LB}|$, at junction B (see Fig. 1). At junction A this load is "seen" through the length h of the second guide, and as h increases it would appear to move on a Smith chart in a clockwise direction around the periphery. A change in h/λ of 0.5 should correspond to a complete revolution. In Fig. 4 we see that for $b = 0.25\lambda$, $\bar{X}_L \approx -2.0$ when $h/\lambda = 0.1$ and when $h/\lambda = 0.6$. The correspondence is not perfect since higher order mode energies play a certain role.

At $b = 0.5\lambda$ the TM_{01} mode in the circular guide can propagate. As h/λ increases, so does $\bar{R}_L$, with a corresponding decrease in the capacitive reactance $\bar{X}_L$, just as with a short monopole.

When $b = 0.75\lambda$ the $\bar{X}_L$ characteristic is almost identical to that for $b = 0.25\lambda$, the cutoff case, possibly because the TM_{02} mode is only slightly below cutoff in the circular guide. This requires a large amount of capacitive stored energy in its field for $z > h$ and with such a large capacitive load reactance at junction B the corresponding load at junction A will again vary greatly as h/λ is changed.

For $b = 1.0\lambda$, both the TM_{01} and TM_{02} modes in the circular guide can propagate; this gives a larger $\bar{R}_L$ (compared with the $b = 0.5\lambda$ case), as well as a more rapidly varying $\bar{X}_L$.

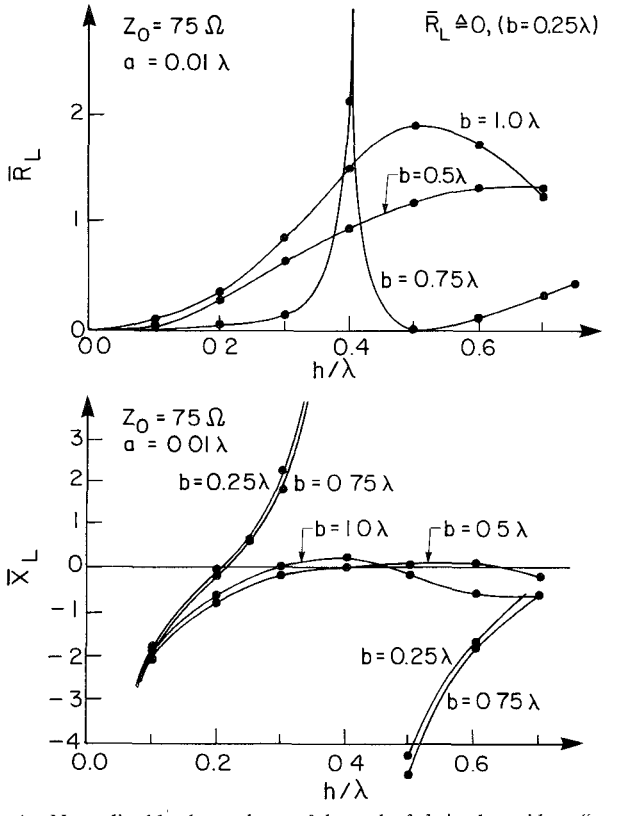

Fig. 4. Normalized load impedance of the probe fed circular guide as "seen" by a coaxial line ($Z_0 = 75\ \Omega$, $a = 0.01\lambda$) as a function probe length h/λ with guide radius b as a parameter.

IV. Conclusion

The conservation of complex power technique is a reliable method for modal analysis of scattering at waveguide junctions [4]–[6]. Our theoretical and experimental results for the present case of a coaxial line probe feeding a circular waveguide indicate that the CCPT can be used for configurations of considerable complexity. Moreover the amount of computation involved, as explained in Section III, is quite reasonable.

Finally, it is important to point out that if the radius of the third guide (see Fig. 1) is increased without limit ($b_3 \to \infty$) then junction B becomes a coaxial line terminated in an infinite ground plane. The scattering matrix $[S_B]$ of such a junction is available [9]. Moreover if the radius b_2 of the second guide in Fig. 1 is then allowed to increase, we have in the limit as $b_2 \to \infty$ a coaxial line feeding a monopole antenna over an infinite conducting ground plane. The CCPT solution to this very interesting and practical problem will be the subject of a paper in the near future.

Appendix
Matrices Used to Determine $[S_A]$ and $[S_B]$

$[E_A]$ (at the Coaxial–Coaxial Junction A)

The E-field mode matching matrix $[E_A]$ at junction A (see Fig. 1) has, for TM_{0q} modes only, as its nmth element:

$$E^A_{nm} = 2\pi \frac{\beta_{1m}\beta_{2n}}{\beta_{1m}^2 - \beta_{2n}^2}\left[\beta_{1m}\rho Z_2(\beta_{1m}\rho) Z_1(\beta_{2n}\rho) - \beta_{2n}\rho Z_1(\beta_{1m}\rho) Z_2(\beta_{2n}\rho)\right]\Big|_a^{b_1} \quad \text{(A1)}$$

where, for $i = 1,2$ and $q = 1,2,\cdots$, β_{iq} satisfies the transcendental equation:

$$J_0(\beta_{iq}b_i) Y_0(\beta_{iq}a) - Y_0(\beta_{iq}b_i) J_0(\beta_{iq}a) = 0 \quad \text{(A2)}$$

and

$$Z_i(\beta_{iq}\rho) = -\frac{\sqrt{\pi}}{2\left\{\left[\frac{J_0(\beta_{iq}a)}{J_0(\beta_{iq}b)}\right]^2 - 1\right\}^{1/2}} \cdot\left[Y_0(\beta_{iq}b_i) J_i(\beta_{iq}\rho) - J_0(\beta_{iq}b_i) Y_i(\beta_{iq}\rho)\right]. \quad \text{(A3)}$$

For those cases involving the TEM or TM_{00} mode, if $N_{i0} = [2\pi \ln(b_i/a)]^{-1/2}$, then

$$E^A_{00} = 2\pi N_{10} N_{20} \ln\left(\frac{b_1}{a}\right) \quad \text{(A4)}$$

$$E^A_{n0} = -2\pi N_{10}\left[Z_0(\beta_{2n}\rho)\Big|_a^{b_1}\right] \qquad E^A_{0m} = 0 \quad \text{(A5)}$$

and

$$Z_0(\beta_{2n}\rho) = \frac{\sqrt{\pi}}{2\left[\frac{J_0^2(\beta_{2n}a)}{J_0^2(\beta_{2n}b)} - 1\right]^{1/2}} \cdot\left[J_0(\beta_{2n}\rho) Y_0(\beta_{2n}a) - J_0(\beta_{2n}a) Y_0(\beta_{2n}\rho)\right]. \quad \text{(A6)}$$

$[E_B]$ (at Coaxial-Circular Waveguide Junction B)

In this case, if $\beta_{3n}b_3$ is the nth root of $J_0(x)$, the E-field mode matching matrix, for TM_{0q} modes only, has as its nmth element:

$$E^B_{nm} = \frac{(\pi/4)^{1/2}\beta_{2m}\beta_{3n}}{\beta_{3n}b_3 J_1(\beta_{3n}b_3)\left(\beta_{2m}^2 - \beta_{3n}^2\right)} \cdot\left[\beta_{2m}\rho J_1(\beta_{3n}\rho) Z_2(\beta_{2m}a) - \beta_{3n}\rho J_2(\beta_{3n}\rho) Z_1(\beta_{2m}b)\right]\Big|_a^{b_2} \quad \text{(A7)}$$

where, for $i = 1,2$ and $m \neq 0$

$$Z_i(x) = \frac{\sqrt{\pi}}{2\left[\frac{J_0^2(\beta_{2m}a)}{J_0^2(\beta_{2m}b)} - 1\right]^{1/2}} \cdot\left[J_i(x) Y_0(\beta_{2m}a) - Y_i(x) J_0(\beta_{2m}a)\right]. \quad \text{(A8)}$$

If $m = 0$, $n = 1,2,\cdots$,

$$E^B_{n0} = \frac{2a\pi^{1/2}N_{20}}{\beta_{3n}b_3 J_1(\beta_{3n}b_3)}\left[J_0(\beta_{3n}b_2) - J_0(\beta_{3n}a)\right]. \quad \text{(A9)}$$

The Line Matrix $[L_2]$

The nmth element of the diagonal line matrix $[L_2]$ used in (1) and (2) is

$$L_{2,nm} = e^{-\gamma_{2m}h}\delta_{nm} \quad \text{(A10)}$$

where γ_{2m} is the propagation constant of the TM_{0m}th mode in guide 2.

Then, as described in detail in [4] and [5], the conservation of complex power technique can be used to obtain the two scattering matrices $[S_A]$ and $[S_B]$.

REFERENCES

[1] J. R. Whinnery, H. W. Jamieson, and T. E. Robbins, "Coaxial-line discontinuities," *Proc. IRE.*, vol. 32, pp. 695–709, Nov. 1944.

[2] E. W. Risley, Jr., "Discontinuity capacitance of a coaxial line terminated in a circular waveguide," *IEEE Trans. Microwave Theory Tech.*, vol. MTT-17, pp. 86–92, Feb. 1969.

[3] E. W. Risley, Jr., "Discontinuity capacitance of a coaxial line terminated in a circular waveguide: Part II—Lower bound solution," *IEEE Trans. Microwave Theory Tech.*, vol. MTT-21, pp. 564–566, Aug. 1973.

[4] R. Safavi-Naini and R. H. MacPhie, "On solving waveguide junction scattering problems by the conservation of complex power technique," *IEEE Trans. Microwave Theory Tech.*, vol MTT-29, pp. 337–343, Apr. 1981.

[5] R. Safavi-Naini and R. H. MacPhie, "Scattering at rectangular-to-rectangular waveguide junctions," *IEEE Trans. Microwave Theory Tech.*, vol. MTT-30, pp. 2060–2063, Nov. 1982.

[6] R. R. Mansour and R. H. MacPhie, "A unified hybrid-mode analysis for planar transmission lines with multilayer isotropic/anisotropic substrates," *IEEE Trans. Microwave Theory Tech.*, vol. MTT-35, pp. 1382–1391, Dec. 1987.

[7] R. Mittra and S. W. Lee, *Analytical Techniques in the Theory of Guided Waves*. New York: Macmillan, 1971.

[8] G. A. Deschamps, "Determination of the reflection coefficients and insertion loss of a waveguide junction," *J. Appl. Phys.*, vol. 24, pp. 1046–1050, Aug. 1953.

[9] T. Do-Nhat and R. H. MacPhie, "On the effect of gap width on the admittance of solid circular cylindrical dipoles," *IEEE Trans. Antennas Propagat*, vol. 37, pp. 1545–1553, Dec. 1989.

An Experimental Technique for *In Vivo* Permittivity Measurement of Materials at Microwave Frequencies

KATIE F. STAEBELL AND DEVENDRA MISRA, MEMBER, IEEE

***Abstract*—This paper involves the formulation of a new procedure to be used in making *in vivo* dielectric measurements with an open-ended coaxial line probe. The theory behind the technique is discussed along with a correction method to account for the system imperfections. Experimental results are compared with the corresponding data available in the literature. The limitations of this technique are considered.**

I. INTRODUCTION

In order to understand the interaction of an electromagnetic field with a material medium, it is important to accurately know its complex permittivity. This information is also desired in many areas of science and engineering, including process control in industries and diagnostic and therapeutic application of microwaves in biomedical engineering. Classical methods of measuring the permittivity of a material require special preparation of a sample that is placed inside a waveguide or cavity and, hence, are not suited for many modern applications. For example, in the case of biological materials, *in vivo* properties are desired. An open-ended coaxial sensor has attracted several researchers because of its applicability in nondestructive measurement over a broad frequency band. However, the relation between the measured reflection coefficient and complex permittivity of the material is not simple. Several attempts have been made to devise a practical way of determining the permittivity from the measured data [1]. Recently, Marsland and Evans reported a bilinear transformation scheme to account for the imperfection in the measuring system in conjunction with an equivalent circuit model for the coaxial opening [2]. However, this technique is restricted at high frequencies by the inadequate circuit model for the probe.

The present approach is based on a quasi-static analysis of the coaxial sensor to formulate a relatively more accurate equivalent model [3], [4]. The experimental results determined by this method are compared with the corresponding values available in the literature over the frequency range of 1 to 20 GHz. The limitations of this technique are also considered.

II. THEORETICAL BACKGROUND

A stationary formula for the aperture admittance of an open-ended coaxial line terminated by a semi-infinite medium on a ground plane is given in [3]. Under a quasi-static approximation, this expression reduces to

$$Y_L \simeq j\frac{2\omega I_1}{[\ln(b/a)]^2}\epsilon^* - j\frac{\omega^3\mu_0 I_2}{[\ln(b/a)]^2}\epsilon^{*2} + \frac{\pi\omega^4\mu_0^{3/2}}{12}\left[\frac{b^2-a^2}{\ln(b/a)}\right]^2\epsilon^{*5/2} \quad (1)$$

where a and b are the inner and outer radii of coaxial aperture, respectively; μ_0 is the permeability of free space; ϵ^* is the complex permittivity of the semi-infinite medium; ω is the angular frequency of electromagnetic fields; and I_1 and I_2 are two triple integrals dependent on the radii but constant otherwise [3]. The medium under consideration is assumed to be linear, isotropic, homogeneous, and nonmagnetic. Other details of this formulation are available in [3] and, therefore, are omitted for the sake of brevity.

The first term of (1) represents a capacitance; the third one, radiation conductance, is used in an equivalent circuit model by several researchers [1], [2]. The second term of this equation represents a frequency-dependent capacitance, which is new and probably responsible for restrictions at high frequencies in the work reported by Marsland and Evans [2]. It is to be noted that this term is important in comparison to the radiation conductance (third term) because of its contribution even around 1 GHz.

III. SYSTEM CALIBRATION

In formulating (1), an infinite conducting flange is assumed over the coaxial aperture. However, it is not used in practice because it is inconvenient. Also, small discontinuities between the aperture and the reflection meter (due to connectors, etc.) cannot be avoided. In order to account for these imperfections, we consider an equivalent two-port network connected between the meter and the coaxial opening. The actual admittance of the aperture terminated by a sample is evaluated from the measured reflection coefficient after calibrating the system with three standard materials as follows [2], [4]:

$$\frac{Y_s - Y_1}{Y_s - Y_2}\cdot\frac{Y_3 - Y_2}{Y_1 - Y_3} = \frac{\delta_{s1}\delta_{32}}{\delta_{s2}\delta_{13}} \quad (2)$$

where Y_s is the desired aperture admittance terminated by the

Manuscript received June 1, 1989; revised October 3, 1989. This work was supported by the National Science Foundation under Grant ECE-8717857.

The authors are with the Electromagnetic Communication Research Laboratory, Department of Electrical Engineering, University of Wisconsin-Milwaukee, P.O. Box 784, Milwaukee, WI 53201.

IEEE Log Number 8933002